Large scale, synchronous variability of marine fish populations driven by commercial exploitation

Kenneth T. Frank[a,b,1], Brian Petrie[a], William C. Leggett[b], and Daniel G. Boyce[b]

[a]Ocean and Ecosystem Sciences Division, Bedford Institute of Oceanography, Dartmouth, NS, Canada B2Y 4A2; and [b]Department of Biology, Queen's University, Kingston, ON, Canada K7L 3N6

Edited by James A. Estes, University of California, Santa Cruz, CA, and approved June 1, 2016 (received for review February 11, 2016)

Synchronous variations in the abundance of geographically distinct marine fish populations are known to occur across spatial scales on the order of 1,000 km and greater. The prevailing assumption is that this large-scale coherent variability is a response to coupled atmosphere–ocean dynamics, commonly represented by climate indexes, such as the Atlantic Multidecadal Oscillation and North Atlantic Oscillation. On the other hand, it has been suggested that exploitation might contribute to this coherent variability. This possibility has been generally ignored or dismissed on the grounds that exploitation is unlikely to operate synchronously at such large spatial scales. Our analysis of adult fishing mortality and spawning stock biomass of 22 North Atlantic cod (*Gadus morhua*) stocks revealed that both the temporal and spatial scales in fishing mortality and spawning stock biomass were equivalent to those of the climate drivers. From these results, we conclude that greater consideration must be given to the potential of exploitation as a driving force behind broad, coherent variability of heavily exploited fish species.

synchrony | fishing mortality | climate forcing | cod

Current wisdom holds that coupled atmosphere–ocean forcing, commonly represented by climate indexes such as the Atlantic Multidecadal Oscillation (AMO) and North Atlantic Oscillation (NAO), is the primary driver of large-scale synchronous variations in the abundance of marine fish populations (1–12). In a recent comprehensive literature review (12) it was concluded that "it is well understood by marine scientists that climate variability is a strong driver of changes in fish populations and in fisheries." Although we do not dispute the potential importance of climate, the possibility that commercial exploitation could contribute significantly to these variations (13–15) has been largely dismissed, the assumption being that fishing mortality could not vary coherently at these scales (2, 16, 17). Other researchers have argued that estimates of exploitation rates often do not exist or are difficult to obtain, thereby limiting the incorporation of such effects into climate-related analyses of fish population dynamics (18). This is not the case for cod in the North Atlantic, a reality that facilitates an evaluation of the hypothesis that fishing pressure may cause synchronous changes in stock abundance at spatial and temporal scales comparable to those attributed to climate forcing (~1,000 km).

Cod has been heavily exploited in the western North Atlantic, where the average instantaneous fishing mortality rate (F) from 1959 to 1993, at which time widespread closures were initiated, was 0.59, corresponding to an annual biomass removal of 43%; in the eastern North Atlantic, even higher levels of exploitation prevailed, with an average F of 0.76 (1961–2012), corresponding to an annual biomass removal of 53%. The large-scale synchronous variability of this widely distributed species has been attributed to climate forcing (19, 20) operating at the scales of ocean basins. These fishing mortality rates are typically three- to six-times greater than the assumed natural mortality rate. The volatile changes in abundance that have characterized the species, coupled with its commercial importance, have led to intensive, long-term monitoring of its population structure and abundance. Consequently, detailed observations of 22 independently managed North Atlantic stocks, whose distributions span 27° of latitude and 97° of longitude, were available with which to investigate the role of exploitation in influencing the temporal and spatial synchrony in abundance (Fig. 1*A*). For each stock, we extracted time series of F from published stock assessments. These series were then used as our index of exploitation (Fig. 1 *B* and *C* and *SI Appendix*, Fig. S1 and Table S1). Time series of spawning stock biomass (SSB) were similarly developed and used to assess the potential of exploitation to induce synchrony in population abundance and the scales at which this synchrony occurred (Fig. 1 *D* and *E* and *SI Appendix*, Fig. S1). The average time-series length was 40 y (range 20–54 y). Annual estimates of F and SSB were available for all 22 stocks from 1984 to 2000.

For the 13 Northwest Atlantic (NWA) cod stocks, the 1982–2000 period featured coherent [median correlation coefficient (r) among stocks = 0.60, range −0.14 to 0.94] variability in the standardized anomalies (z scores) of F with an intense and rapidly developing peak in the late 1980s to early 1990s (Fig. 1*B*). Standardized F increased at the annual rate of +0.4 during the interval 1987–1992; this corresponds to an increase in the annual removal of cod biomass from 35% in 1987 to 66% in 1992. This increase in the rate of exploitation was followed by a precipitous decline in the abundance of the 13 stocks (Fig. 1*D*) from a combined SSB of 1.5 million tons in 1987 to 0.4 million tons in 1993. A similar pattern occurred before 1982, when data for fewer stocks were available. At that time, a pronounced peak in F occurred in the early to mid-1970s and was followed by a sharp decline in SSB just before the establishment of the 200-nautical mile limit in 1977.

Significance

Large-scale synchronous variation in the abundance of marine fish populations has generally been viewed as a response to coupled atmosphere–ocean forcing. The possibility that commercial exploitation could contribute significantly to these variations has been largely dismissed. We demonstrate, using data from 22 Atlantic cod stocks distributed across the North Atlantic, that fishing pressure can cause synchronous changes in stock abundance at spatial and temporal scales comparable to those attributed to climate forcing. We conclude that an understanding of the underlying causes of the large-scale, often synchronous variability of exploited marine fish populations and their underlying food chains will require greater acceptance of the potential importance of exploitation than has been evident to date.

Author contributions: K.T.F. designed research; K.T.F., B.P., W.C.L., and D.G.B. performed research; K.T.F., B.P., W.C.L., and D.G.B. analyzed data; and K.T.F., B.P., and W.C.L. wrote the paper.

The authors declare no conflict of interest.

This article is a PNAS Direct Submission.

Data deposition: The raw data used in this paper can be found in *SI Appendix*, Fig. S1 and the locations of the data are listed in *SI Appendix*, Table S1.

[1]To whom correspondence should be addressed. Email: kenneth.frank@dfo-mpo.gc.ca.

This article contains supporting information online at www.pnas.org/lookup/suppl/doi:10.1073/pnas.1602325113/-/DCSupplemental.

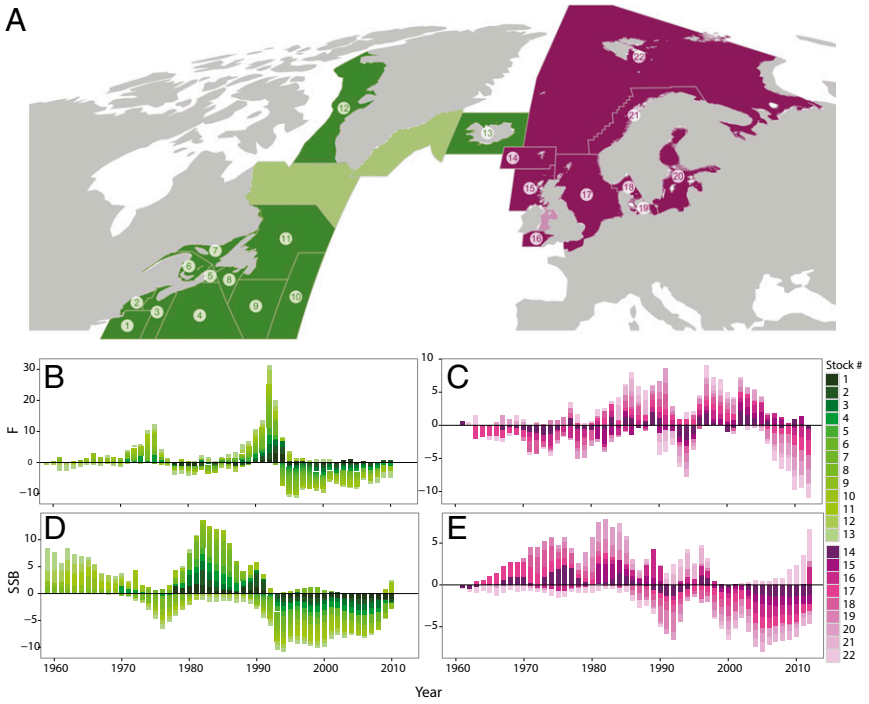

Fig. 1. Cod populations in the North Atlantic and associated fishing mortality and SSB. (*A*) Locations of North Atlantic cod stocks: 1: 5Z, Georges Bank; 2: 5Y, Gulf of Maine; 3: 4X, Western Scotian Shelf/Bay of Fundy; 4: 4VsW, Eastern Scotian Shelf; 5: 4Vn, Sydney Bight; 6: 4T, Southern Gulf of St. Lawrence; 7: 3Pn4RS, Northern Gulf of St. Lawrence; 8: 3Ps, Southern Newfoundland Shelf; 9: 3NO, Southern Grand Bank; 10: 3M, Flemish Cap; 11: 2J3KL, Hamilton Bank/Northeast Newfoundland Shelf/Northern Grand Bank; 12: West Greenland; 13: Iceland/East Greenland; 14: Faroes; 15: West Scotland; 16: Celtic Sea; 17: North Sea; 18: Kattegat; 19: Western Baltic; 20: Central Baltic; 21: Northeast Arctic Coastal; 22: Northeast Arctic/Barents Sea. Unnumbered colored regions lack analytical assessments of cod. (*B–E*) Stacked times series of Northwest Atlantic *F* (*B*) and SSB (*D*) anomalies and Northeast Atlantic *F* (*C*) and SSB (*E*) anomalies. For each stock and year, *F* and SSB values were standardized and the anomaly was calculated according to $V_i^s = (V_i - V_{Ave})/V_{SD}$, where V_i represents either *F* or SSB in year *i*, the superscript s represents the standardized anomaly, and Ave is the average value for a particular stock.

For the nine Northeast Atlantic (NEA) cod stocks, the pattern of standardized anomalies of F was less coherent ($r = 0.14$; range −0.45 to 0.77) (Fig. 1*C*). However, a general increase in coherence did occur through time, with 8 of 9 stocks exhibiting positive standardized *F* anomalies in 1986, 1987, and 1989, contributing to a broad peak. A second, stronger peak in *F* occurred from 1997 to 1999, when all nine stocks had positive anomalies. Each peak in *F* was followed by coherent declines in SSB (Fig. 1*E*). Between these peaks, six of nine stocks had average *F* anomalies with the same sign. A period of strong decline in standardized *F* (0.16 y^{-1}; total −2.4) occurred between 1997 and 2012. In real terms, average *F* declined from 0.97 y^{-1} (1997; 61% biomass removal) to 0.47 y^{-1} (2012; 38% removal).

The coherent behavior of *F* and SSB (Fig. 1 *B–E*) prompted us to consolidate the cod stocks into two large units representing the NW and NE Atlantic (Fig. 2). In both the NWA and NEA, SSB and *F* were negatively correlated (Fig. 2). The response to increased *F* in year y typically was a decline in SSB in year y+1 (*SI Appendix*, Fig. S2), as seen in the NWA from the early 1980s to the early 1990s (Fig. 2*A*). In 1992, a moratorium on directed fishing for cod was declared for stock 11 and, in 1993, similar management measures were implemented for stocks 4–7 and 9. However, by 1994, the NWA stocks had moved from this nearly linear response and become fixed in a state where low *F* did not lead to a significant response in SSB. Several hypotheses have been advanced to explain the lack of cod recovery, including increased natural mortality, alterations in critical demographic characteristics, reduced recruitment rates, and bycatch in open fisheries (21). On the other hand, in the NEA, decreasing *F* led to increasing cod stocks overall from the late 1980s to 2010–2012; this evolution was dominated by the NE Arctic stock (*SI Appendix*, Fig. S1). In both the NWA and NEA the cod stocks moved along linear trajectories, with R^2 and slopes of 0.73 and −2.0 million tons per unit *F* for the NWA (1970–1993) and 0.61 and −1.8 million tons per unit *F* for the NEA (1966–2012). The weaker, but not significantly different, slope for the NEA may reflect the generally higher temperatures experienced by these stocks leading to greater growth and resilience to excessive fishing pressure or a more balanced fishery, where forage and top predator species are simultaneously harvested. Despite experiencing similar fishing mortalities, the NEA did not become fixed in a low *F*/low SSB state; rather, recent estimates of SSB are the highest over the length of the time series (Fig. 2*B*).

It is evident that these series are dominated by low-frequency variability, with zero crossings of the autocorrelation function ranging from 6 to greater than 14 y (*SI Appendix*, Fig. S3); further, about 40–70% of the variance is found at periods greater than 10 y. This concentration of variance at long timescales implies few degrees of freedom, which could lead to significant uncertainty in the interpretation of any statistical relationships between potential forcing mechanisms, such as fishing pressure or climate, and response variables, such as SSB (18). Conclusions that might be drawn regarding cause and effect could therefore be compromised.

A general picture of the spatial structure and temporal variability of exploitation was derived from a principal component analysis (PCA) based on the correlation matrix of *F* for the complete time series of 22 North Atlantic cod stocks (*Materials and Methods* and Fig. 3). Synchronous variability of *F* among stocks would be reflected as strong, in-phase (same-sign) loadings with similar amplitudes over a large area. Nonsynchronous behavior would feature a more random distribution of the amplitudes and signs of the loadings. Complementary analyses involved the calculation of PCAs

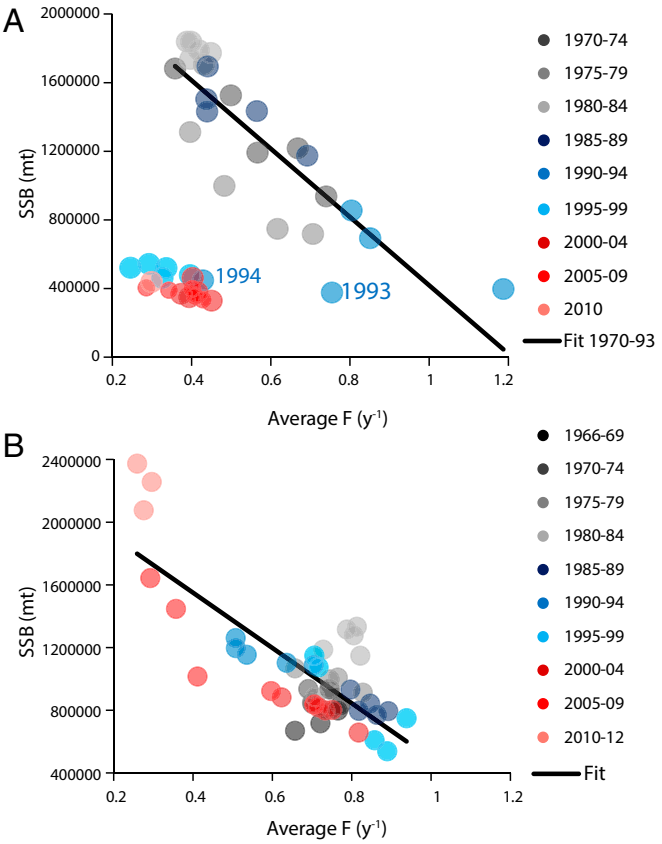

Fig. 2. Comparison of the *F* values in year y and the response to this level of exploitation represented by SSB in year y+1 for the (*A*) NW and (*B*) NE Atlantic. The 13 (NW) and 9 (NE) SSB of cod stocks were combined, as were the *F* estimates, to represent two integrated stocks for the North Atlantic. Given that exploitation generally affects the following year's biomass, we compared *F* in year y with SSB in the following year, y+1. The data are color-coded in 5-y blocks to allow the temporal evolution of SSB and *F* to be seen.

based on 1984–2000 data, when all 22 series were complete, intercomparisons of PCAs based on the correlation and covariance matrices, and intercomparisons of time series of the PCAs with the average *F* time series (*Materials and Methods* and *SI Appendix*, Figs. S4–S7). Based on the correlation matrix alone, we expected a high level of synchrony among stocks, given that the average correlation coefficient was 0.43 (95% confidence interval 0.38–0.48) and that 73 of 114 (64%) interstock correlation coefficients exceeded $r = 0.37$, a threshold value defined in a subsequent analysis for estimating the spatial scale of synchrony.

The two leading PCA components extracted 56% of the overall variance in *F* and operated at the scale of ∼1,000 km. The first mode (PCA 1) (Fig. 3*A*) captured 36% of the overall variance. Its spatial structure was dominated by strong, in-phase loadings for all North American, West Greenland, and Icelandic stocks that span 4,000 km. The loadings for these NWA stocks had similar amplitudes (coefficient of variation or CV 23%) and were on average 3.3 times larger than the amplitudes of their NEA counterparts. The time series of the leading mode (PCA 1) was reflective of the average value of *F* for the 13 NWA stocks (*SI Appendix*, Fig. S5 *A* and *C*). In turn, this accounts for most of the temporal variability in SSB ($r = -0.85$; 1970–1993) and was characterized by the development of two pronounced peaks (Fig. 3*C*). The first peak occurred in the mid-1970s, coincident with intensive, largely unregulated, foreign overfishing. The large offshore trawler fleets of these nations operated over vast geographic areas spanning multiple cod stock management units across Northwest Atlantic Fisheries Organization divisions 1–5 (West Greenland to Georges Bank). From 1960 to 1976, landings of cod by foreign fleets amounted to 78% from a total of 20.6 million tons; Canada was responsible for the remaining 22%. In contrast, the second peak in the early 1990s arose primarily from the rapid rise and expansion of domestic fishing effort following the implementation of extended jurisdiction to 200 nautical miles in 1977. Canada's share of the total cod landings (9.4 million tons) during the period 1977–1993 rose to 70%. Many of the cod stocks collapsed following the second peak, and were placed under fishing moratoria with limited recovery to date (Figs. 1*D* and 2*A*).

In sharp contrast to the unimodal distribution of the fishing mortality to which these NWA cod stocks were subjected, and to its corresponding effect on SSB, NWA sea surface (22) and bottom (23) temperatures were characterized by a strong bimodal spatial distribution, the boundary separating positive and negative temperature anomalies being located on the northeast Scotian Shelf (stock 4) (Fig. 1*A*). PCA 1 also featured generally weaker, negative (i.e., out-of-phase) loadings (Fig. 3*A*) for NEA stocks, perhaps reflecting the bimodal basin-scale temperature response to the NAO, the dominant driver of atmospheric variability in the region (24), which results in temperature anomalies on the Newfoundland/Labrador Shelf having opposite signs to those over much of the European shelf (*SI Appendix*, *Section F* and Figs. S8 and S9 contain further discussion and analysis of the spatial dependence of SSB response on large-scale forcing and the use of local time series of environmental forcing).

The second mode (PCA 2) (Fig. 3*B*) captured 20% of the overall variance of *F* and featured in-phase loadings for eight of nine NEA stocks and for the Icelandic stock; the loadings of these eight NEA stocks had similar amplitudes (CV 33%). The loadings were generally weak among the NWA stocks. These results are strongly indicative of synchronous temporal variability in *F* across eight of nine NEA stocks over a scale of ∼2,000 km. This coherent behavior of the loadings was somewhat less pronounced in the NEA (less proportional variance accounted for, greater CV, eight of nine stocks) relative to the NWA (Fig. 3*A*). The time series of the second leading mode (PCA 2) (Fig. 3*C*) was reflective of the average value of *F* for the nine NEA stocks (*SI Appendix*, Fig. S5 *B* and *D*), which in turn accounted for a significant amount of the temporal variability in SSB ($r = -0.74$) (Fig. 2*B*). The time series was characterized by a prolonged period of high exploitation from the 1970s to early 1990s, resulting in an increasing proportion of stocks falling to biomass levels below precautionary levels (25). A declining trend in exploitation has been evident since the early 2000s and, combined with the near abolishment of illegal, unreported, and unregulated fishing, some cod stocks have been showing signs of major improvement (26). On the other hand, a recent study (27) suggested that the trends in abundance and distribution of Northeast Arctic cod (stock 22) (Fig. 1*A*), which accounts for 56% on average of the total NEA stock since 1984 and 79% in the last decade, are related to the direct and indirect effects of temperature on stock dynamics. However, the rise of ocean temperature by ∼1 °C that accompanied the dramatic increase of cod by nearly 2 million tons from the late 1990s to the present may well be confounded with the reduction of *F* from 1.07 in 1997 to 0.25 in 2010 (*SI Appendix*, Fig. S1).

To address the possibility that these findings were not the result of attributing *F* to possible time-varying natural mortality (M), we repeated these analyses using an alternative measure of exploitation, relative *F* [defined as landings per SSB (28)]. Virtually identical results were obtained (*SI Appendix*, Fig. S7). We do recognize that our alternative measure using catch data was part of the estimation method that was used to generate SSB. Therefore, we also developed a time series of exploitation for a subset (total of five) of stocks based on fishery-independent survey estimates of relative biomass and compared it with the corresponding model-derived *F*

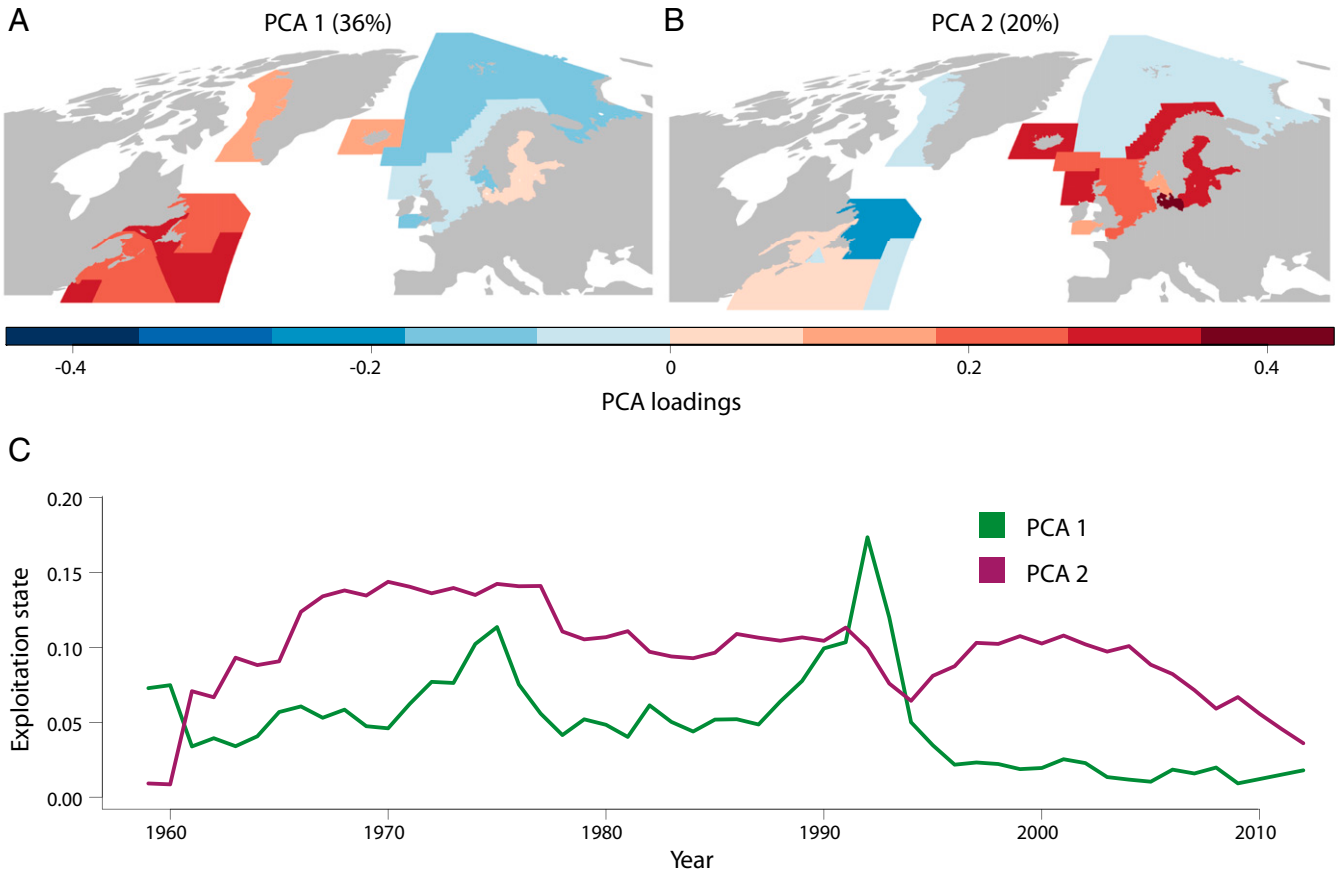

Fig. 3. (*A* and *B*) Loadings based on a PCA of the correlation matrix of *F* for (*A*) PCA 1 and (*B*) PCA 2. (*C*) The changing pattern of exploitation pressure on cod based on the time series of the two leading modes from the PCA (PCA 1 and PCA 2) representative of the western and eastern Atlantic stocks, respectively.

series (*SI Appendix*, *Section G*). In all cases, a positive relationship was obtained with an average R^2 of ~0.6 (*SI Appendix*, Fig. S10).

An explicit determination of how coherence in *F* and SSB decayed with distance was achieved by calculating all possible pairs of lag-0 correlations among NWA and NEA cod stocks as a function of the distance (kilometers) between the centers of each stock's distributions. The groupings for each region were based on the PCA loadings (Fig. 3 *A* and *B*). The derived scales depended on the mathematical form of the exponential decay model used [e.g., the ratio of the longest to shortest scale was 1.9 for NWA *F* (1,680 vs. 3,330 km) and 1.1 for NWA SSB (1,890 vs. 2,150 km)]; consequently, an empirical method was devised to estimate the spatial scale (*Materials and Methods*). We found that the spatial scales over which *F* was coherent, expressed as the distance at which the correlation falls to $e^{-1} = 0.37$ (commonly referred to as the e-folding scale), were 790 km for the NWA and 610 km for the NEA (Fig. 4 *A* and *B* and *SI Appendix*, Fig. S11). The corresponding scales for SSB were 1,050 km for the NWA and 720 km for the NEA (Fig. 4 *C* and *D* and *SI Appendix*, Fig. S11). These scales are comparable to those of climate forcing in the NWA and NEA (22–24, 29–31). Thus, these analyses reveal that, contrary to the prevailing assumption (2, 16, 17), the scales of fishing mortality are equivalent to those of atmosphere–ocean forcing, and could account for a significant portion of the large-scale synchrony that prevails in these cod stocks.

The characterization of *F* and SSB was further evaluated by focusing on an assessment of temporal scales. We conducted a Fourier analysis of the time series of *F* and SSB as well as the AMO (1960–2014) and NAO (1960–2014), the two climate drivers most commonly implicated in the dynamics of North Atlantic fish populations (10). All series were rich in low-frequency energy (*SI Appendix*, Fig. S12). The median periods (i.e., the point at which the integral of the amplitude spectrum is equally divided) were NWA *F* 6.3 y, SSB 7.7 y and NEA *F* 6.6 y, SSB 7.4 y. The median periods for the climate drivers were AMO 7.1 y and NAO 4.9 y. This similarity among the median temporal periods of the climate indexes *F* and SSB makes it difficult to distinguish the relative roles of exploitation and climate as regulators of open-ocean stock variability. Moreover, it indicates that the dominant variability in the biological and abiotic variables is concentrated at low frequencies, leading to few degrees of freedom in the available time series, which could complicate the understanding of the roles of climate and direct anthropogenic impacts on ecosystems.

A major factor giving rise to the dominance of low-frequency variability in *F* arises from management practices that take the form of the setting of the annual total allowable catch (TAC) for each of the cod stocks. To illustrate this point, we assembled time series of TACs for 10 NWA and 8 NEA cod stocks and calculated their autocorrelations (*SI Appendix*, Fig. S13). For the NWA stocks, six did not cross 0 for lags of up to 10 y, whereas two crossed at ~3 y (stocks 4 and 5; implying a dominant period of about 12 y) and 2 at 4 y (stocks 9 and 13; equal to a dominant period of about 16 y). For the eight NEA stock TACs, six did not cross 0 for lags of up to 10 y, whereas two crossed or approached 0 at about 4 y (*SI Appendix*, Fig. S13, *Lower*). The inherent sluggishness in the adjustment of the TACs reflects attempts to limit variability in interannual changes in the management of the fishery, but has the troubling side effect of not responding quickly enough when a stock is in decline.

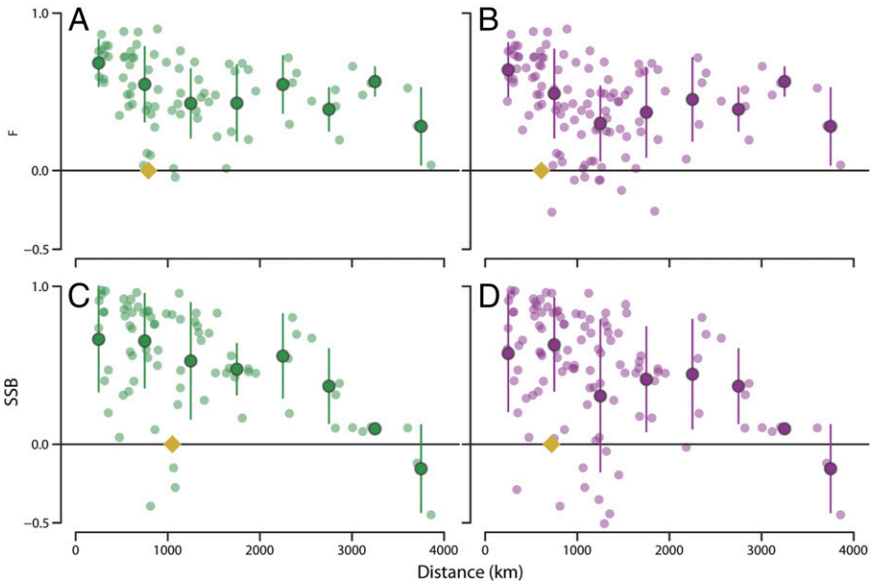

Fig. 4. Spatial scales of fishing mortality and spawning stock biomass for North Atlantic cod stocks. Interstock correlations, based on the Pearson product–moment correlation, are shown as a function of separation between the centers of cod stock areas for (*A*) *F* for the 13 NWA stocks, (*B*) F for the 9 NEA stocks, (*C*) SSB NWA, and (*D*) SSB NEA. Individual interstock correlations are represented by light color circles; the dark circles with vertical lines represent average correlations in 500-km blocks with SE and are plotted at the average separation of points within the 500-km block. The last block covers more than 500 km to obtain sufficient points for averaging. The diamond shape intersecting the *x* axis shows the e-folding distance. For the NWA, 77% and 73% of the interstock correlations in *F* and SSB, respectively, were >0.37 (=e^{-1}); a similar comparison for the NEA revealed that 36% and 56% were >0.37.

Collectively, our findings raise serious questions about the attribution of environmental forcing in the variability of marine fish populations that currently prevails. Marginalization of nonclimatic factors, including fishing pressure, was common in a review of over 250 case studies involving climate change effects on the temporal dynamics of marine populations (18). Whereas previous research has focused heavily on the role of climate as the driver of large-scale synchrony of marine fish populations (4–11), our analyses demonstrate that fishing pressure can also exert strong effects on the population trajectories of cod at spatial and temporal scales comparable to those of climate forcing. This documentation of the potential synchronizing effect of large-scale industrial fishing on the targeted populations of cod adds to the growing number of examples in which human activities could have induced homogenization of formerly spatially diverse populations and the systems they inhabit, for example through artificial propagation (31), invasive species, and habitat transformations (32).

We conclude that a more comprehensive understanding of the underlying causes of the large-scale and often synchronous variability of exploited marine fish populations, and the food chains leading to their production, will require a greater acceptance of the potential importance of exploitation than has been evident to date and a more rigorous assessment of the relative roles of both climate and exploitation. Clearly, if the results of our analyses can be generalized, and until it has been definitively shown that they cannot, the focus on climate that has prevailed in recent decades can no longer be accepted without considering commercial exploitation, particularly given the significance of the marine capture fisheries to the global economy.

Materials and Methods

Annual estimates of instantaneous fishing mortality, spawning stock biomass, and commercial landing data were obtained for 22 cod stocks distributed throughout the North Atlantic. Additionally, data were obtained for two large-scale environmental indexes: the AMO and NAO (*SI Appendix*, Table S1). Our primary objective involved characterization of the spatial and temporal scales of variability in *F*, SSB, and the environmental indexes. This was achieved in multiple analytical ways. We first used PCA using all of the available data from 1959 to 2013 (73% data coverage) to construct a correlation matrix of *F* in addition to the period (1984–2000) when all stocks had data and the matrix was fully balanced. This allowed maximum use of all of the time series, series that varied substantially in length (minimum 24 y, maximum 54 y, average 40 y) and overlap. Because this approach can give rise to negative eigenvalues and invalid results, we compared the results derived from the full matrix with results from a matrix derived from the period 1984–2000 (*SI Appendix*, Fig. S4), when there was full coverage. To generate time series for the leading principal components, we averaged the output by the number of sites where there were data. An additional PCA was carried out to determine whether decomposition based on the covariance matrix rather than the correlation matrix offered any additional or different insight (*SI Appendix*, Fig. S6). We next determined the spatial scales associated with the total variability by computing the correlations for all possible stock pairs based on the *F* and SSB time series. Guided by the PCA results, we divided the data into western and eastern North Atlantic groups and determined the scales for *F* and SSB. We considered three regression models to fit the variation of the correlation with separation (*X*) between stocks: A*exp(–*BX*), where A was allowed to vary or set equal to 1, and A*ln(*x*) + *B*. In addition, we adopted an empirical approach. This involved ordering the data by the separation between stocks from the smallest to largest distance. The average (Ave) correlation and its SE were computed for the first 10 points; if (Ave − SE), which represents a confidence interval of 84%, was greater than e^{-1}, the block was advanced one point and the computation was repeated until (Ave − SE) was less than e^{-1}. The spatial scale was then defined as the greatest separation in the last block for which (Ave − SE) was greater than e^{-1}: that is, the e-folding scale. Finally, the temporal variability in *F* and SSB for western and eastern Atlantic stocks as well the two large-scale environmental indexes under consideration (AMO and NAO) were evaluated by conducting a Fourier analysis of the respective time series using the MATLAB routine fft (MathWorks); the results are displayed as amplitude spectra. Additional analysis considered multiple inputs with SSB as the response variable and *F*, NAO, and AMO series as potential drivers.

ACKNOWLEDGMENTS. We thank J. A. D. Fisher, D. Gillis, and N. L. Shackell for helpful comments and suggestions on an earlier draft of the manuscript, and the reviewers (including M. Fogarty) for insightful comments that led to further analyses and improvements to the manuscript. Support for this research was provided by Fisheries and Oceans Canada and NSERC Discovery grants (to K.T.F. and W.C.L.).

1. Botsford LW, Castilla JC, Peterson CH (1997) The management of fisheries and marine ecosystems. *Science* 277(5325):509–515.
2. Megrey BA, et al. (2009) A cross-ecosystem comparison of spatial and temporal patterns of covariation in the recruitment of functionally analogous fish stocks. *Prog Oceanogr* 81(1–4):63–92.
3. Noakes DJ, Beamish RJ (2009) Synchrony of marine fish catches and climate and ocean regime shifts in the North Pacific Ocean. *Mar Coast Fish* 1(1):155–168.
4. Garrod DJ, Colebrook JM (1978) Biological effects of variability in the North Atlantic Ocean. *Int Council Exploration Sea* 173:128–144.
5. Koslow JA (1984) Recruitment patterns in Northwest Atlantic fish stocks. *Can J Fish Aquat Sci* 41(12):1722–1729.
6. Koslow JA, Thompson KR, Silvert W (1987) Recruitment to Northwest Atlantic cod (*Gadus morhua*) and haddock (*Melanogrammus aeglefinus*) stocks: Influence of stock size and climate. *Can J Fish Aquat Sci* 44(1):26–39.
7. Garrod DJ, Schumacher A (1994) North Atlantic cod: The broad canvas. *ICES Mar Sci Symp* 198:59–76.
8. Rothschild BJ (2007) Coherence of Atlantic cod stock dynamics in the Northwest Atlantic Ocean. *Trans Am Fish Soc* 136(3):858–874.
9. Brunel T, Boucher J (2007) Long-term trends in fish recruitment in the North-East Atlantic related to climate change. *Fish Oceanogr* 16(4):336–349.
10. Drinkwater KF, et al. (2014) The Atlantic Multidecadal Oscillation: Its manifestation and impacts with special emphasis on the Atlantic region north of 60° N. *J Mar Syst* 133:117–130.
11. Rouyer T, Fromentin J-M, Hidalgo M, Stenseth NC (2014) Combined effects of exploitation and temperature on fish stocks in the Northeast Atlantic. *ICES J Mar Sci* 71(7):1554–1562.
12. Lehodey P, et al. (2006) Climate variability, fish, and fisheries. *J Clim* 19(20): 5009–5030.
13. Myers RA, Barrowman NJ, Thompson KR (1995) Synchrony of recruitment across the North Atlantic: An update. (Or, "now you see it, now you don't!") *ICES J Mar Sci* 52(1): 103–110.
14. Worm B, Myers RA (2004) Managing fisheries in a changing climate. *Nature* 429(6987):15.
15. Minto C, Mills Flemming J, Britten GL, Worm B (2014) Productivity dynamics of Atlantic cod. *Can J Fish Aquat Sci* 71(2):203–216.
16. Conversi A, et al. (2015) A holistic view of marine regime shifts. *Philos Trans R Soc B* 370(1659):20130279.
17. Beaugrand G, et al. (2015) Synchronous marine pelagic regime shifts in the Northern Hemisphere. *Philos Trans R Soc B* 370(1659):20130272.
18. Brown CJ, et al. (2011) Quantitative approaches in climate change ecology. *Glob Change Biol* 17(12):3697–3713.
19. Brander K, Mohn R (2004) Effect of the North Atlantic Oscillation on recruitment of Atlantic cod (*Gadus morhua*). *Can J Fish Aquat Sci* 61(9):1558–1564.
20. Stige LC, Ottersen G, Brander K, Chan KS, Stenseth NC (2006) Cod and climate: Effect of the North Atlantic Oscillation on recruitment in the North Atlantic. *Mar Ecol Prog Ser* 325:227–241.
21. Shelton PA, Sinclair AF, Chouinard GA, Mohn R, Duplisea DE (2006) Fishing under low productivity conditions is further delaying recovery of Northwest Atlantic cod (*Gadus morhua*). *Can J Fish Aquat Sci* 63(2):235–238.
22. Thompson KR, Loucks RH, Trites RW (1988) Sea surface temperature variability in the shelf-slope region of the Northwest Atlantic. *Atmos-Ocean* 26(2):282–299.
23. Petrie B (2007) Does the North Atlantic Oscillation affect hydrographic properties on the Canadian Atlantic continental shelf? *Atmos-Ocean* 45(3):141–151.
24. Visbeck M, et al. (2003) in *The North Atlantic Oscillation: Climatic Significance and Environmental Impact*, eds Hurrell JW, Kushnir Y, Ottersen G, Visbeck M (Am Geophys Union, Washington, DC), pp 113–145.
25. Garcia SM, De Leiva Moreno JI (2005) Evolution of the state of fish stocks in the Northeast Atlantic within a precautionary framework, 1970–2003: A synoptic evaluation. *ICES J Mar Sci* 62(8):1603–1608.
26. Kjesbu OS, et al. (2014) Synergies between climate and management for Atlantic cod fisheries at high latitudes. *Proc Natl Acad Sci USA* 111(9):3478–3483.
27. Hollowed AB, Sundby S (2014) Change is coming to the northern oceans. *Science* 344(6188):1084–1085.
28. Sinclair AF (1998) Estimating trends in fishing mortality at age and length directly from research survey and commercial catch data. *Can J Fish Aquat Sci* 55(5): 1248–1263.
29. Cayan DR (1986) *North Atlantic Seasonal Sea Surface Temperature Anomalies and Associated Statistics, 1949–1985* (Scripps Inst Oceanogr, La Jolla, CA), Rep 85-19.
30. Polyakova E, Journel A, Polyakov I, Bhatt U (2006) Changing relationship between the North Atlantic Oscillation and key North Atlantic climate parameters. *Geophys Res Lett* 33(3):L03711.
31. Moore JW, McClure M, Rogers LA, Schindler DE (2010) Synchronization and portfolio performance of threatened salmon. *Conserv Lett* 3(5):340–348.
32. Rahel F (2007) Biogeographic barriers, connectivity and homogenization of freshwater faunas: It's a small world after all. *Freshw Biol* 52(4):696–710.